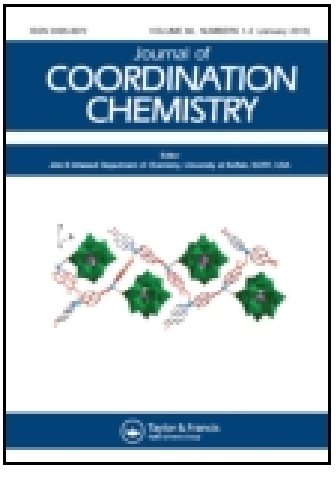

Journal of Coordination Chemistry
Publication details, including instructions for authors and subscription information:
http://www.tandfonline.com/loi/gcoo20

Synthesis and characterization of Cu^{II}-Ln^{III} (Ln = Ho, Tm, Yb, or Lu) complexes with N_2O_4-donor Schiff base ligand

Beata Cristóvão[a], Julia Kłak[b] & Barbara Miroslaw[c]

[a] Faculty of Chemistry, Department of General and Coordination Chemistry, Maria Curie-Sklodowska University, Lublin, Poland

[b] Faculty of Chemistry, University of Wrocław, Wrocław, Poland

[c] Faculty of Chemistry, Department of Crystallography, Maria Curie-Sklodowska University, Lublin, Poland

Accepted author version posted online: 28 Jul 2014.Published online: 03 Sep 2014.

To cite this article: Beata Cristóvão, Julia Kłak & Barbara Miroslaw (2014) Synthesis and characterization of Cu^{II}-Ln^{III} (Ln = Ho, Tm, Yb, or Lu) complexes with N_2O_4-donor Schiff base ligand, Journal of Coordination Chemistry, 67:16, 2728-2746, DOI: 10.1080/00958972.2014.948432

To link to this article: http://dx.doi.org/10.1080/00958972.2014.948432

Journal of Coordination Chemistry, 2014
Vol. 67, No. 16, 2728–2746, http://dx.doi.org/10.1080/00958972.2014.948432

Synthesis and characterization of Cu^{II}–Ln^{III} (Ln = Ho, Tm, Yb, or Lu) complexes with N_2O_4-donor Schiff base ligand

BEATA CRISTÓVÃO*†, JULIA KŁAK‡ and BARBARA MIROSLAW§

†Faculty of Chemistry, Department of General and Coordination Chemistry, Maria Curie-Sklodowska University, Lublin, Poland
‡Faculty of Chemistry, University of Wrocław, Wrocław, Poland
§Faculty of Chemistry, Department of Crystallography, Maria Curie-Sklodowska University, Lublin, Poland

(*Received 4 March 2014; accepted 26 June 2014*)

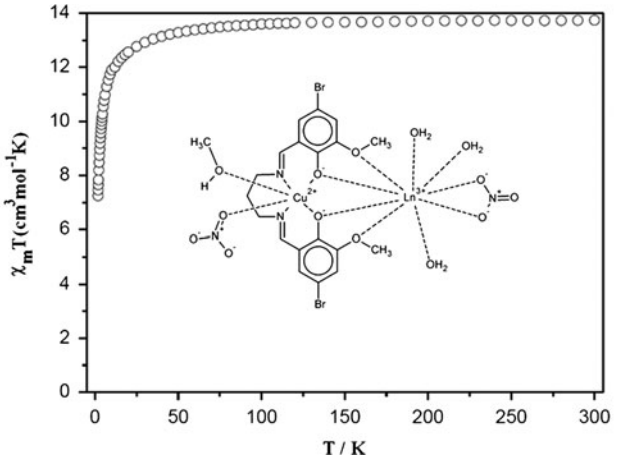

The heterodinuclear compounds $[CuLn(L)(NO_3)_2(H_2O)_3MeOH]NO_3 \cdot MeOH$ (where Ln = Ho (**1**), Tm (**2**), Yb (**3**), and Lu (**4**)) have been synthesized and characterized by elemental analysis, FTIR, TG/DSC, TG-FTIR, single crystal X-ray diffraction studies, and magnetic measurements. The complexes are isostructural and crystallize in the monoclinic space group $P2_1/n$. The magnetic properties of **1**, **2**, and **3** are dominated by the crystal field effect on the Ln^{III} site, masking the magnetic interaction between the paramagnetic centers.

The heterodinuclear complexes $[CuLnL(NO_3)_2(H_2O)_3MeOH]NO_3 \cdot MeOH$ (Ln = Ho (**1**), Tm (**2**), Yb (**3**), and Lu (**4**); L = *N,N′*-bis(5-bromo-3-methoxysalicylidene)propylene-1,3-diamine) have been synthesized and characterized by elemental analysis, FTIR, thermogravimetric (TG)/differential scanning calorimetry (DSC), TG-FTIR, single crystal X-ray diffraction studies, and magnetic measurements. The isostructural compounds crystallized in the monoclinic space group $P2_1/n$. The rare earth(III) cation is nine coordinate, whereas the coordination number for copper(II) is six. The complexes were stable at room temperature. The thermal decomposition products were mainly CH_3OH, H_2O, CH_3Br, NO_x ($x = 1$ or 2), CO_2, and CO. The magnetic properties of **1–3** were

*Corresponding author. Email: beata.cristovao@poczta.umcs.lublin.pl

dominated by the crystal field effect on the Ln^{III} site, masking the magnetic interaction between the paramagnetic centers. The Cu^{II}–Lu^{III} pair in **4** showed no significant interaction, which is in accord with the diamagnetic nature of the ground state for lutetium(III).

Keywords: Heterodinuclear complexes; Schiff base; 3d–4f Compound; Magnetic properties

1. Introduction

The application of N,O-donor Schiff base compounds as ligands for complexation with 3d and 4f metal cations is an interesting research area of coordination chemistry. Investigations of Cu^{II}–Ln^{III} heteronuclear complexes mainly focused on the correlations between molecular structure and magnetic properties [1–7]. The first study of the magnetic properties of a heterometallic 3d–4f compound was reported by Gatteschi *et al.* who reported the ferromagnetic interaction between Cu^{II} and Gd^{III} ions [1]. The preliminary studies were limited to Cu^{II}–Gd^{III} complexes, because this metal combination is expected to be ferromagnetic. For other 3d–4f coordination compounds, the magnetic properties are still difficult to predict due to various factors such as thermal population of the Stark components of Ln^{III}, the interactions between Cu^{II}–Ln^{III} ions, the stereochemistry of the complexes, and masking effects. Kahn *et al.* predicted theoretically that coupling of $4f^n$ ions with paramagnetic species should be antiferromagnetic for Ln^{III} ions with less than seven 4f electrons and ferromagnetic for $n \geq 7$ [2]. However, examples of complexes reported subsequently do not fully corroborate this prediction. Koner *et al.* investigated a series of heterodinuclear Cu^{II}–Ln^{III} Schiff base complexes $[M^{II}L^1Ln^{III}(NO_3)_3]$, where H_2L^1 = *N,N′*-ethylenebis (3-ethoxysalicylaldiimine), Ln^{III} from Ce^{III} to Yb^{III}, and reported that there are antiferromagnetic interactions between Cu^{II} and Ln^{III} ions for the lanthanide cations from the beginning of the 4f series (Ce^{III}, Nd^{III}, Sm^{III}), whereas the Cu^{II}–Pr^{III} and Cu^{II}–Eu^{III} pairs behave as spin-uncorrelated systems. Ferromagnetic interactions occur from Gd^{III} toward the end of the 4f series (except for Er^{III}) [3]. Studies of Costes *et al.* for magnetic properties of heterodinuclear compounds $[CuL(Me_2CO)Ln(NO_3)_3]$, where L = dideprotonated form of {2,2′-[1-methyl-1,2-propanediylbis(nitrilomethylidyne]-di(6-methoxyphenol)}, show antiferromagnetic exchange interaction between Cu^{II}–Ln^{III} ions for Ln = Ce^{III}, Nd^{III}, and Sm^{III}, as well as for Tm^{III} and Yb^{III}. Ferromagnetic behavior was reported for Ln = Gd^{III}, Tb^{III}, Dy^{III}, Ho^{III}, and Er^{III}; whereas Cu^{II}–Pr^{III}, Cu^{II}–Eu^{III}, Cu^{II}–La^{III}, and Cu^{II}–Lu^{III} analogs are devoid of any significant interaction [4]. Elmali *et al.* investigated Cu^{II}–Dy^{III} complex ($L^2Cu(Me_2CO)Dy(NO_3)_3$, L^2 = *N,N′*-bis(2-hydroxy-3-methoxybenzylidene)-ethylenediamine, and stated that the magnetic properties of this compound are dominated by the crystal field effect on the Dy^{III} site, masking the magnetic interaction between the paramagnetic centers [5]. Kahn *et al.* studied oxamato-bridged Cu^{II}–Ln^{III} complexes having a general formula $\{Ln_2[M(opba)]_3\}\cdot S$, where opba = *ortho*-phenylenebis-(oxamato) and *S* = solvent. They observed ferromagnetic interaction for Gd^{III}, Tb^{III}, and Dy^{III} and perhaps for Tm^{III}, whereas antiferromagnetic interaction between Ln^{III} and Cu^{II} ions was reported for other lanthanides (Ce^{III}, Pr^{III}, Nd^{III} Sm^{III}, Er^{III}, Ho^{III}, and Yb^{III}) [6]. Jana *et al.* studied a series of Schiff base complexes having formulas $[Cu^{II}LLn^{III}(NO_3)_3(H_2O)]$ (Ln = Ce–Nd), $[Cu^{II}LLn^{III}(NO_3)_3]\cdot CH_3COCH_3$ (Ln=Sm), $[Cu^{II}(H_2O)LLn^{III}(NO_3)_3]$ (Ln = Eu, Gd), and $[Cu^{II}LLn^{III}(NO_3)_3]$ (Ln=Sm, Tb–Yb) (H_2L was obtained on condensation of 3-ethoxysalicylaldehyde with *trans*-1,2-diaminocyclohexane). They reported that the metal centers in the Cu^{II}–Tb^{III}, Cu^{II}–Dy^{III}, Cu^{II}–Ho^{III}, Cu^{II}–Er^{III}, and Cu^{II}–Tm^{III} compounds are coupled by

ferromagnetic interaction, whereas the Cu^{II}−Yb^{III} complex shows antiferromagnetic interaction. In the series of light lanthanide(III) complexes, the pairs of ions Cu^{II}–Ce^{III}, Cu^{II}−Pr^{III}, Cu^{II}−Nd^{III}, and Cu^{II}−Sm^{III} exhibit antiferromagnetic interactions, whereas the Cu^{II}–Eu^{III} complex behaves as a spin-uncorrelated system [7].

N,N′-bis(5-bromo-3-methoxysalicylidene)propylene-1,3-diamine ($H_2L = C_{19}H_{20}N_2O_4Br_2$) (further abbreviated to BMSPDA) as a hexadentate ligand has an inner smaller site (N_2O_2) with two nitrogens and two μ-phenoxo oxygens ligating to 3d metal cation and an outer bigger one (O_2O_2) with two μ-phenoxo and two methoxy oxygens coordinating the lanthanide [8–16]. Ions of rare earth elements behave as hard acids and prefer oxygen to nitrogen donors, whereas 3d metal ions can coordinate to both nitrogens and oxygens. Yang *et al.* synthesized a homotrinuclear complex $[Zn_3L_2(NO_3]\cdot MeOH$ using BMSPDA and zinc nitrate. The coordination spheres of the two zinc cores located in the inner N_2O_2 cavities of the Schiff base ligands adopt distorted square pyramidal geometries. The zinc occupying the central position is coordinated by four phenolic and two methoxy oxygens. This compound crystallizes in the monoclinic space group $P2_1/c$ [8]. The reaction of the above complex with Yb^{III} salt yields the heterotetrametallic complex $[Zn_2Yb_2L_2(\mu\text{-}OH)_2Cl_4]\cdot 2MeCN$ with interesting luminescent properties. The complex crystallizes in the triclinic space group *P*-1. Each Yb^{III} ion is coordinated by four oxygens O_2O_2 from the outer Schiff base cavity, two bridging hydroxides, and one chloride. Each five-coordinate Zn^{II} ion occupies the inner N_2O_2 cavity of the Schiff base ligand [8]. Yang *et al.* reported also a hexanuclear luminescent Zn^{II}–Nd^{III} compound $[Zn_4Nd_2L_4(1,4\text{-}BDC)_2]\cdot[Nd(NO_3)_5(H_2O)]\cdot Et_2O\cdot 2EtOH\cdot 3H_2O$ (where BDC is 1,4-benzenedicarboxylate) that crystallizes in the triclinic space group *P*-1. The complex was obtained from the reaction of zinc acetate, neodymium nitrate, BMSPDA, and BDC in ethanol [9]. Each 10-coordinate Nd^{III} ion is surrounded by eight oxygens from two Schiff bases and two oxygens from bridging carboxylates of BDC. The five-coordinate zinc ions are bound inside the N_2O_2 cavities of Schiff base ligands [9]. Starting from the same BMSPDA Schiff base, we have synthesized mononuclear, heterodi-, heterotri-, and heterotetranuclear compounds of Cu^{II}, Ni^{II}, and Cu^{II}/Ni^{II}–Ln^{III} with different structures and physicochemical properties [10–16]. The complexes have the following formulas: $[CuL\subset(H_2O)]$, $[NiL(H_2O)_2]$, $[CuLn(L)(NO_3)_2(H_2O)_3MeOH]NO_3\cdot MeOH$ (Ln = Gd, Tb, Dy, Er), $[Cu_2Ln(L)_2(NO_3)(H_2O)_2](NO_3)_2\cdot 3H_2O$ (Ln = La, Ce, Pr, Nd, Sm, Eu) $[Ni_2Ln(L)_2(CH_3COO)_2(MeOH)_2]NO_3\cdot 4H_2O$ (Ln = La, Ce, Pr, Nd) $[Cu_2La_2(L)_2(NO_3)_6(EtOH)_2]$, and $[Ni_2Gd_2(L)_2(CH_3COO)_2(NO_3)_2](NO_3)_2\cdot 6H_2O\cdot 4MeOH$. The heterotrinuclear compounds Cu^{II}–Ln^{III}−Cu^{II} crystallize in the monoclinic space group $C2/c$ [10, 11], whereas the Ni^{II}–Ln^{III}–Ni^{II} complexes crystallize in the $P2_1/n$ one [12, 13]. In both types of complexes, the lanthanide(III) ion lies on the inversion center, and the inner salen-type cavity N_2O_2 is occupied by copper(II) or nickel(II). The lanthanide(III) cation is present in the open and larger O_2O_2 compartment. The coordination number of Ln^{III} is ten, of Cu^{II} is five, and of Ni^{II} is six. In the obtained heterotrinuclear compounds, each pair of 3d-4f ions is linked by two bridging phenoxo oxygens of the Schiff base ligand and, additionally in the case of Ni^{II}–Ln^{III}−Ni^{II} by one acetate ion [10–13]. The dinuclear complexes Cu^{II}–Ln^{III} crystallize in the monoclinic space group $P2_1/n$ [10, 14]. The Cu^{II} and Ln^{III} ions are bridged via two phenolic oxygens from BMSPDA. In these compounds, the Ln^{III} is nine coordinate and Cu^{II} is six coordinate [10, 14]. The inert heterotetranuclear complex $[Cu_2La_2L_2(NO_3)_6(EtOH)_2]$ crystallizes in the monoclinic space group $P2_1/c$ with only half of the molecule in the asymmetric unit. Similar to trinuclear compounds, the inner N_2O_2 salen-type cavity is also occupied by transition metal (five-coordinated Cu^{II} ion) whereas ten-coordinate La^{III} is present in the open, larger O_2O_2 space of the Schiff base ligand [15]. The

nitrate-bridged $[Ni_2Gd_2(L)_2(CH_3COO)_2(NO_3)_2](NO_3)_2\cdot 6H_2O\cdot 4MeOH$ complex crystallizes in the monoclinic $P2_1/c$ space group. The Gd^{III} and Ni^{II} cations of the tetranuclear core are linked by phenoxy oxygens from the Schiff base ligand and by nitrates. The gadolinium (III) ion is nine coordinate and nickel has a coordination number of six [16]. The mononuclear inclusion compound $[CuL\subset(H_2O)]$ with four-coordinate Cu^{II} occupying the N_2O_2 cavity and water molecule encapsulated through O–H···O hydrogen bonds in the O_2O_2 compartment crystallizes in the triclinic space group *P*-1 [15]. The mononuclear $[NiL(H_2O)_2]$ crystallizes in orthorhombic space group *Pnma* with the molecule lying on the mirror plane. Ni^{II} has octahedral coordination and occupies the N_2O_2 cavity of the organic ligand. Water molecules from the apical positions of the nickel coordination sphere form hydrogen bonds to four oxygens from the empty O_2O_2 cavity [12]. These studies show how various coordination architectures can be obtained using the same Schiff base ligand, but changing the metal ions and synthesis conditions. The temperature-dependent magnetic susceptibilities, from 1.8 to 300 K, and the field-dependent magnetization indicate that in the studied 3d-4f heterodi- and heterotrinuclear compounds of BMSPDA, the interaction between transition metal (Cu^{II} or Ni^{II}) and lanthanide(III) ions is antiferromagnetic for Ce, Pr, and Nd and ferromagnetic for Gd, Tb, Dy, and Er [10–16], fully in accord with Kahn's assumptions.

In the present paper, we report the synthesis, structure, and characterization of heterodinuclear compounds $[CuLn(L)(NO_3)_2(H_2O)_3MeOH]NO_3\cdot MeOH$ (where Ln = Ho (**1**), Tm (**2**), Yb (**3**), and Lu (**4**), $L = C_{19}H_{18}N_2O_4Br_2$) with *N,N′*-bis(5-bromo-3-methoxysalicylidene) propylene-1,3-diamine (BMSPDA).

2. Experimental

2.1. *Materials*

The reagents 5-bromo-2-hydroxy-3-methoxybenzaldehyde, 1,3-diaminopropane, $Cu(CH_3COO)_2\cdot H_2O$, $Ho(NO_3)_3\cdot 5H_2O$, $Tm(NO_3)_3\cdot 5H_2O$, $Yb(NO_3)_3\cdot 5H_2O$, $Lu(NO_3)_3\cdot xH_2O$, and solvent MeOH used for synthesis were commercially available from Aldrich Chemical Company and Polish Chemical Reagents. They were used as received.

2.2. *Synthesis*

$[CuLn(L)(NO_3)_2(H_2O)_3MeOH]NO_3\cdot MeOH$ (Ln = Ho (**1**), Tm (**2**), Yb (**3**), and Lu (**4**)).

The *N,N′*-bis(5-bromo-3-methoxysalicylidene)propylene-1,3-diamine (H_2L) and heterodinuclear compounds **1–4** were prepared according to the procedure described earlier [14]. A mixture of the Schiff base (H_2L) (0.4 mM, 0.1999 g) in MeOH (20 mL) and $Cu(CH_3COO)_2\cdot H_2O$ (0.4 mM, 0.0799 g) was stirred at room temperature for 30 min, while a freshly prepared 5 mL methanol solution of Ln(III) nitrate ($Ho(NO_3)_3\cdot 5H_2O$ (0.2 mM, 0.0882 g); $Tm(NO_3)_3\cdot 5H_2O$ (0.2 mM, 0.0890 g); $Yb(NO_3)_3\cdot 5H_2O$ (0.2 mM, 0.0898 g); $Lu(NO_3)_3\cdot xH_2O$ (0.2 mM, 0.0722 g) was added. Then the resulting green mixture was stirred for another 30 min, followed by filtration. Green single crystals suitable for X-ray structure analysis were formed at low temperature (4 °C) by slow evaporation of the filtrates after several weeks. We have failed to obtain well-shaped crystals of Lu^{III} complex **4**.

$[CuHo(L)(NO_3)_2(H_2O)_3MeOH]NO_3\cdot MeOH$ (**1**); Yield: 105 mg/52%. Elemental analysis for $C_{21}H_{32}N_5O_{18}Br_2CuHo$ (1030.80). Calcd (%): C, 24.45; H, 3.10; N, 6.79; Cu, 6.16; Ho, 16.00. Found (%): C, 24.63; H, 2.90; N, 6.74; Cu, 6.20; Ho, 15.60.

[CuTm(L)$(NO_3)_2(H_2O)_3$MeOH]NO_3·MeOH (**2**); Yield: 108 mg/54%. Elemental analysis for $C_{21}H_{32}N_5O_{18}Br_2CuTm$ (1034.80). Calcd (%): C, 24.35; H, 3.09; N, 6.76; Cu, 6.14; Tm, 16.32. Found (%): C, 24.75; H, 2.90; N, 6.74; Cu, 6.00; Tm, 16.30.

[CuYb(L)$(NO_3)_2(H_2O)_3$MeOH]NO_3·MeOH (**3**); Yield: 105 mg/52%. Elemental analysis for $C_{21}H_{32}N_5O_{18}Br_2CuYb$ (1038.91). Calcd (%): C, 24.25; H, 3.08; N, 6.74; Cu, 6.12; Yb, 16.65. Found (%): C, 23.93; H, 2.74; N, 6.38; Cu, 6.25; Yb, 16.40.

[CuLu(L)$(NO_3)_2(H_2O)_3$MeOH]NO_3·MeOH (**4**); Yield: 110 mg/55 %. Elemental analysis for $C_{21}H_{32}N_5O_{18}Br_2CuLu$ (1040.84). Calcd (%): C, 24.40; H, 3.10; N, 6.78; Cu, 6.15; Lu, 16.94. Found (%): C, 24.75; H, 2.57; N, 6.30; Cu, 6.30; Lu, 16.45.

2.3. *Methods*

The carbon, hydrogen, and nitrogen contents in the compounds were determined by elemental analysis using a CHN 2400 Perkin Elmer analyzer.

The copper and lanthanide contents were established using an ED XRF spectrophotometer (Canberra-Packard).

FTIR spectra of complexes were recorded from 4000 to 400 cm^{-1} using an M-80 spectrophotometer (Carl Zeiss Jena). Samples for FTIR spectra measurements were prepared as KBr disks.

The magnetization of the Cu^{II}–Ln^{III} (Ln^{III} = Ho, Tm, Yb, and Lu) powdered samples was measured from 1.8 to 300 K using a Quantum Design SQUID-based MPMSXL-5-type magnetometer. The superconducting magnet was generally operated at a field strength ranging from 0 to 5 T. Measurements were made at magnetic field 0.5 T. The SQUID magnetometer was calibrated with a palladium rod sample. Corrections are based on subtracting the sample – holder signal and contribution χ_D estimated from Pascal's constants.

Thermal analyses of the prepared compounds were carried out by the thermogravimetric (TG) and differential scanning calorimetry (DSC) methods using the SETSYS 16/18 analyzer (Setaram). The experiments were carried out under air flow from 20 to 1000 °C at a heating rate of 10 °C min^{-1}. The samples (7.74 mg (**1**), 7.54 mg (**2**), 7.80 mg (**3**), and 7.68 mg (**4**)) were heated in Al_2O_3 crucibles.

The TG–FTIR coupled measurements have been carried out using a Netzsch TG apparatus coupled with a Bruker FTIR IFS66 spectrophotometer. Samples of about 10 mg were heated to 800 °C (compounds) and 900 °C (Schiff base), respectively, at a heating rate of 10 °C min^{-1} in flowing argon atmosphere.

2.4. *X-ray crystal structure determination*

Crystal data for **1** were collected on an Oxford Diffraction Xcalibur Atlas Gemini ultra diffractometer with monochromated CuK_α radiation (λ = 1.54184 Å) at 100(2) K and for **2–4**, on an Oxford Diffraction Xcalibur CCD diffractometer with graphite-monochromated MoK_α radiation (λ = 0.71073 Å) at 290 K. Data-sets were collected using the ω scan technique. The programs CrysAlis CCD and CrysAlis Red [17] were used for data collection, cell refinement, and data reduction. The low quality of data collected for **4** enabled only to determine the space group and unit cell parameters. Analytical absorption correction based on indexing of crystal faces was applied for **1–3** [18]. The structures were solved by direct methods using SHELXS-97 and refined by full-matrix least-squares on F^2 using SHELXL-97 [19] (both operating under WinGX [20]). Non-hydrogen atoms except for two disordered bridging carbons were refined with anisotropic displacement parameters. C9 and C10 of the

propyl bridge in all structures are disordered over two positions with sof's for the major part being 0.51(2), 0.53(2), and 0.53(3) in **1**(Ho), **2** (Tm), and **3** (Yb), respectively. Hydrogens from methanol were found in the difference Fourier maps and refined isotropically. Hydrogens attached to water were refined isotropically with $U_{iso} = 1.5\ U_{eq}$ of oxygen. All remaining hydrogens were positioned geometrically and allowed to ride on their parent, with $U_{iso}(H) = 1.5\ U_{eq}(C_{methyl})$ and $1.2\ U_{eq}$ for other carbons.

3. Results and discussion

3.1. *Infrared spectra*

FTIR spectra of heterodinuclear compounds **1–4** were compared with the spectrum of the free Schiff base H_2L to obtain information about binding mode of the ligand to metal ions (table 1). Schiff bases are capable of forming coordinate bonds with many metal ions through azomethine as well as phenolic groups. The strong and sharp bands due to the azomethine group ν(C=N) of free H_2L at 1636 cm^{-1} were redshifted to 1628 cm^{-1} in spectra of the complexes [21–25]. This feature may be explained by the withdrawing of electrons from nitrogen to copper(II) due to coordination, indicating the involvement of the azomethine nitrogen in formation of metal–ligand bonds and is consistent with the X-ray diffraction results. The metal–nitrogen coordination is also confirmed by the new band at 448 cm^{-1} observed in spectra of complexes and may be assigned to ν(Cu–N) [26, 27]. The Schiff base ligand also coordinates metal ions via deprotonated phenolic oxygen. The phenolic

Table 1. Selected spectroscopic data of the Schiff base (BMSPDA) and $Cu^{II}Ho^{III}$ (**1**) and $Cu^{II}Tm^{III}$ (**2**), $Cu^{II}Yb^{III}$ (**3**), $Cu^{II}Lu^{III}$ (**4**) complexes.

H_2L	1	2	3	4	Proposed assignments
3442*w*	3426*m*	3426*m*	3426*m*	3426*m*	ν(O–H), ν(C–H)
2940*w*	2928*w*	2928*w*	2928*w*	2928*w*	$\nu_{as}(CH_3)$
2872*w*	–	–	–	–	ν(C–H(O))
2844*w*	2848*w*	2848*w*	2848*w*	2848*w*	$\nu_s(CH_3)$
1636*vs*	1628*vs*	1628*vs*	1628*s*	1628*vs*	ν(C=N)
1576*w*	1556*w*	1560*w*	1560*w*	1560*w*	ν(C=C)
1476*vs*	1468*s*	1476*s*	1476*s*	1476*s*	ν(C=C) + $\nu(N–O)_{complex}$
–	1384*vs*	1384*vs*	1384*vs*	1384*vs*	ν(N–O)
1320*m*	–	–	–	–	δ(O–H)
–	1292*vs*	1292*vs*	1292*vs*	1292*vs*	ν(C–O) + $\delta(O–H)_{methanol}$
1252*vs*	1240*m*	1240*m*	1240*m*	1240*m*	ν(C–O)
1096*m*	1096*w*	1096*w*	1096*w*	1096*w*	δ (C–H)
1068*m*	1072*m*	1072*m*	1072*m*	1072*m*	δ(C–H) + $\nu(N–O)_{complex}$
1016*m*	1012*w*	1012*w*	1012*w*	1012*w*	ν(C=C)
968*m*	966*w*	966*w*	966*w*	966*w*	γ(C–H)
864*m*	852*w*	852*w*	852*w*	852*w*	γ(C–H), δ(CCC)
836*m*	820*w*	820*w*	820*w*	820*w*	γ(C–H)
–	792*m*	792*m*	792*m*	792*m*	δ(N–O)
756*m*	762*w*	762*w*	762*w*	762*w*	γ(C–H)
684*w*	696*w*	696*w*	696*w*	696*w*	δ(CCC)
–	632*w*	632*w*	632*w*	632*w*	γ(C–H) + δ(C=C)
–	572*m*	572*m*	572*m*	572*m*	ν(M–O)
–	540*w*	540*w*	540*w*	540*w*	γ(C–H)
–	448*m*	448*m*	448*m*	448*m*	ν(M–N)

Note: *vs* – very strong, *s* – strong, *m* – medium, *w* – weak, ν – stretching, δ – deformation in plane, γ – deformation out of plane, *as* – asymmetric, *sym* – symmetric.

O–H deformation band, δ(O–H), observed in the FTIR spectrum of free ligand at 1320 cm^{-1} did not occur in spectra of **1–4**. Additionally, on complexation, the strong phenolic stretching vibration ν(C–O) at 1252 cm^{-1} in H_2L shifted to lower frequencies in heteronuclear compounds at 1240 cm^{-1}, confirming the involvement of the phenolic oxygen in the metal–ligand bonding. A medium broad band with maximum at 3426 cm^{-1} present in the FTIR spectra of complexes indicates the OH stretching vibrations, ν(O–H), of coordination water and methanol [21, 26, 28]. The weak bands at 2940 and 2840 cm^{-1}, occurring in spectra of the Schiff base and **1–4**, may be assigned to asymmetric and symmetric stretching vibrations of $\nu(CH_3)$ group from *methoxy* substituent [29, 30]. Nitrate ions can coordinate as monodentate, bidentate-chelating (symmetrical or asymmetrical), or bidentate-bridging ligands [31–40]. Sometimes, the separation in IR spectra between the two highest frequency bands characteristic for vibration of coordinated NO_3 group can be used as a criterion to determine the degree of covalence of the nitrate coordination bonding. The values obtained for bidentate nitrate (~180–200 cm^{-1}) are higher compared to those for monodentate (~100–115 cm^{-1}) [33, 38, 39]. The results of the X-ray analysis indicated that monodentate and bidentate chelating, as well as free nitrates were present in **1–4**. In the FTIR spectra of these compounds, the characteristic frequencies of coordinating mono- and bidentate nitrate (both are of C_{2v} symmetry [31, 32]) overlapped and appeared at 1476–1468, 1292, 1072, and 972 cm^{-1}. It is very difficult to determine on the basis of infrared spectroscopy alone what kind of coordination mode exists in **1–4**. The strong band at 1384 cm^{-1} appeared only in spectra of the complexes corresponding to vibrations of uncoordinated (free) nitrate ν(N–O) [27, 33, 35, 38–41]. In the low-frequency regions, the new band observed at 572 cm^{-1} can be attributed to ν(M–O) vibration [26, 27].

3.2. *Crystal and molecular structure*

The heterodinuclear compounds $[CuLn(L)(NO_3)_2(H_2O)_3MeOH]NO_3 \cdot MeOH$ (where Ln = Ho (**1**), Tm (**2**), Yb (**3**), and Lu (**4**)) were isostructural and crystallized in the monoclinic space group $P2_1/n$. The crystal structure with atom-numbering scheme of **1** is shown in figure 1(a) (atom-numbering scheme is analogous for **2** and **3**). The schematic diagram of dinuclear complexes is given in figure 1(b). The crystallographic data and experimental details are summarized in table 2. The selected bond distance and angle values for **1**, **2**, and **3** are presented in table 3. As shown in figure 1, the inner, smaller cavity (N_2O_2) of the Schiff base ligand is occupied by Cu^{II}, whereas the outer, larger (O_2O_2) by Ln^{III} ion. The Cu^{II} and Ln^{III} ions were connected by a double bridge involving two phenolate oxygens (figures 1 and 2). The lanthanide(III) was nine coordinate. Its coordination sphere built of one Schiff base ligand (4O) and one chelating nitrate (2O) was supplemented by three water molecules (3O). The Ln–O distances depended on the chemical nature of the O donors (methoxy, nitrate, aqua, or phenoxo), varying from 2.279(7) Å for Yb1–O5(aqua) to 2.519(7) Å for Yb1–O3(methoxy) (table 3). The six-coordinate copper(II) center adopted a distorted octahedral geometry (figures 1 and 2). Two oxygens and two nitrogens from the Schiff base ligand built the deformed square base. The two oxygens at the apical positions (one from methanol molecule and one from monodentate nitrate) formed longer bonds (2.554(4)–2.626(9) Å). The Cu1, Ln1, O1, and O2 were nearly coplanar. The dihedral angle between the Cu1O1O2 and Ln1O1O2 planes (δ) was *ca.* 3° in **1–3**. As depicted in figure 3, the molecules formed layers perpendicular to the *c* crystallographic axis. The crystal structures of the studied compounds were stabilized by expanded intermolecular hydrogen bonds (C–H···O/N, C–H···π) (table 4).

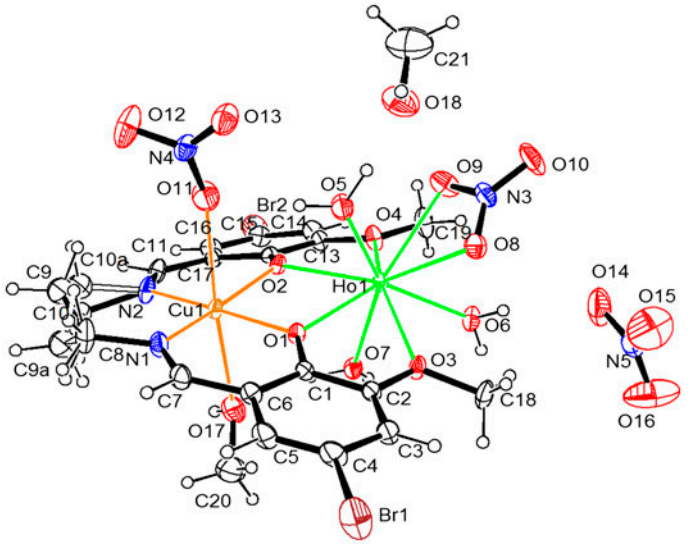

Figure 1(a). The crystal structure with atom-numbering scheme of **1** (displacement ellipsoids were drawn at 30% probability level).

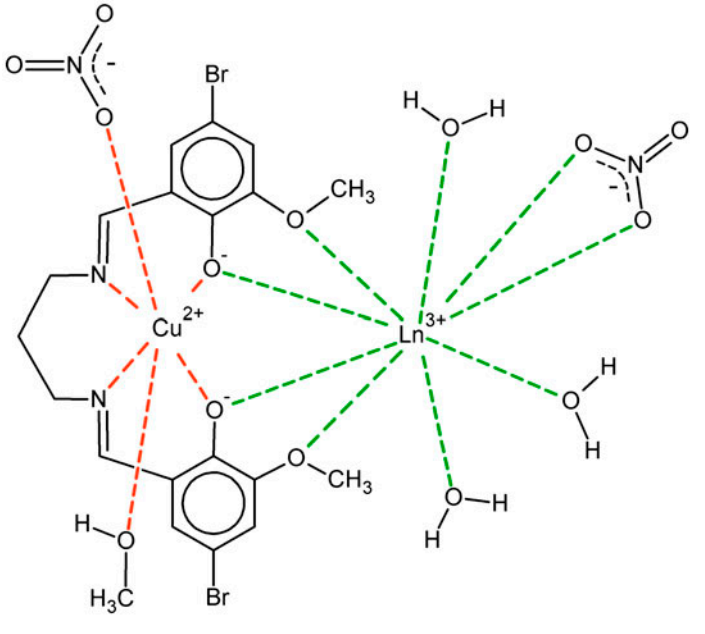

Figure 1(b). Schematic diagram of heterodinuclear Schiff base complexes.

Compounds **1–4** are isostructural with previously reported dinuclear complexes of Cu^{II} and Gd^{III}, Tb^{III} [14], Dy^{III} or Er^{III} ions ($n \geq 7$) [10]. Analogously, synthesized complexes of the first half of the lanthanide row ($n < 7$) (La^{III}, Ce^{III}, Pr^{III}, Nd^{III}, Sm^{III},

Table 2. Crystal data and structure refinement parameters for **1–4**.

	1	**2**	**3**	**4**
Empirical formula	$C_{21}H_{32}N_5O_{18}Br_2CuHo$	$C_{21}H_{32}N_5O_{18}Br_2CuTm$	$C_{21}H_{32}N_5O_{18}Br_2CuYb$	$C_{21}H_{32}N_5O_{18}Br_2CuLu$
Formula weight	1030.80	1034.80	1038.91	1040.84
Crystal system	Monoclinic	Monoclinic	Monoclinic	Monoclinic
Space group	$P2_1/n$	$P2_1/n$	$P2_1/n$	$P2_1/n$
Wavelength (Å); T (K)	1.5418; 100	0.71073; 290	0.71073; 290	0.71073; 290
a (Å)	9.946(1)	9.948(1)	9.914(1)	9.89(2)
b (Å)	16.816(1)	16.855(1)	16.801(2)	16.77(2)
c (Å)	20.177(1)	20.208(1)	20.188(4)	20.40(2)
β (°)	90.67(1)	90.70(1)	90.95(2)	91.7(1)
Volume (Å^3)	3374.4(4)	3388.1(4)	3362.2(8)	3381(7)
Color, shape	Green, prism	Green, prism	Green, prism	Green, plate
Z, calculated density (g cm^{-3})	4; 2.029	4; 2.029	4; 2.052	–
Absorption coefficient (mm^{-1})	8.529	5.670	5.856	–
Absorption correction	Analytical	Analytical	Analytical	–
F (0 0 0)	2012	2020	2024	–
Crystal size (mm)	0.42 × 0.30 × 0.20	0.40 × 0.25 × 0.20	0.40 × 0.25 × 0.20	0.40 × 0.30 × 0.15
Reflections coll./ independ.	62531/6015 [R_{int} = 0.0767]	8184/4972 [R_{int} = 0.0250]	13087/6072 [R_{int} = 0.0705]	–
Data/ parameters	6015/439	4972/439	6072/439	–
Goodness-of-fit on F^2	0.966	1.080	1.045	–
Final R indices [$I > 2\sigma(I)$]	R_1 = 0.0450, wR_2 = 0.1236	R_1 = 0.0341, wR_2 = 0.0780	R_1 = 0.0586, wR_2 = 0.1280	–
Extinction coefficient	0.0039(3)	–	–	–
Max and min $\Delta\rho$ (e Å^{-3})	1.69 and −1.22	1.21 and −0.96	2.51 and −1.31	–

and Eu^{III}) form trinuclear coordination compounds with Cu^{II}–Ln^{III}–Cu^{II} cores and two Schiff base ligands for one molecular unit. They crystallize in the monoclinic space group $C2/c$ [10, 11].

Selected structural parameters of dinuclear complexes Cu^{II}–Ln^{III} (Ln = Gd, Tb, Dy, Ho, Er, Tm, or Yb) derived from BMSPDA and those of the similar reported dinuclear diphenoxo-bridged Schiff base compounds are presented in table 5 [3, 7, 10, 14, 42–45]. In the series of complexes, the bond distances of copper(II) and lanthanide(III) with bridging phenolate oxygens (Cu–O_{phen}, Ln–O_{phen}) *ca.* 1.90 Å and 2.30 Å, respectively, were significantly different. Such differences in bond distances are expected due to their differences in ionic size and are observed in 3d–4f compounds. The geometrical parameters in the coordination environment of the lanthanide center in the all analyzed complexes were similar. The intramolecular copper–lanthanide bond lengths decreased with the increase of the atomic number of lanthanides due to lanthanide contraction.

Table 3. Selected bond lengths, angles, intra-, and intermolecular distances in **1–3** (Å, °).

Bond/distance [Å]	1	2	3	Angle [°]	1	2	3
Ln1–O1	2.351(3)	2.338(4)	2.315(7)	Cu1–O1–Ln1	108.7(1)	108.6(2)	107.9(3)
Ln1–O2	2.356(3)	2.344(4)	2.318(6)	Cu1–O2–Ln1	107.4(1)	107.1(2)	108.8(3)
Ln1–O3	2.516(3)	2.519(4)	2.519(7)	O1–Cu1–Ln1	39.5(1)	39.4(1)	39.1(2)
Ln1–O4	2.490(3)	2.485(4)	2.482(6)	O2–Cu1–Ln1	39.9(1)	39.9(1)	39.4(2)
Ln1–O5	2.329(3)	2.304(4)	2.279(7)	O1–Cu1–N2	168.1(2)	168.0(2)	167.5(3)
Ln1–O6	2.355(3)	2.338(4)	2.323(6)	O2–Cu1–N2	92.7(2)	92.8(2)	93.1(3)
Ln1–O7	2.348(3)	2.316(3)	2.313(7)	O2–Cu1–O1	79.3(1)	79.2(2)	78.5(3)
Ln1–O8	2.437(3)	2.430(4)	2.415(8)	N1–Cu1–O1	92.5(1)	92.6(2)	92.8(3)
Ln1–O9	2.485(4)	2.469(4)	2.474(8)	N1–Cu1–O2	166.5(2)	166.5(2)	165.7(3)
Cu1–O1	1.952(3)	1.954(4)	1.953(6)	N1–Cu1–N2	97.0(2)	96.9(2)	97.2(4)
Cu1–O2	1.983(3)	1.991(4)	1.976(6)	N1–Cu1–Ln1	130.6(1)	130.6(2)	130.5(3)
Cu1–N1	1.987(4)	1.994(5)	1.988(9)	N2–Cu1–Ln1	132.3(1)	132.3(2)	132.3(3)
Cu1–N2	1.967(4)	1.966(5)	1.952(9)	δ	2.7(1)	3.0(2)	2.9(4)
Cu1–O11	2.554(4)	2.560(5)	2.554(8)				
Cu1–O17	2.597(4)	2.603(5)	2.626(9)				
Ln1···Cu1	3.504(1)	3.494(1)	3.476(1)				
Ln1···Cu1^{i}	7.577(1)	7.595(1)	7.574(2)				

Note: Ln1 = Ho1 for **1**, Tm1 for **2**, and Yb1 for **3**; symmetry code: ^{i} $x + 3/2$, $y + 1/2$, $-z + 1/2$; δ – dihedral angle between the Cu1O1O2 and Ln1O1O2 planes.

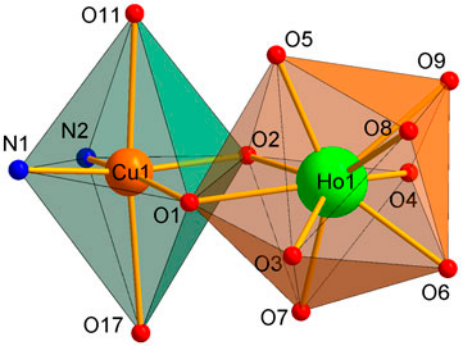

Figure 2. Coordination polyhedra for Ho^{III} and Cu^{II} in the crystal **1**.

3.3. *Magnetic properties*

For each heteronuclear compound Cu^{II}–Ln^{III} (Ln^{III} = Ho (**1**), Tm (**2**), Yb (**3**), or Lu (**4**)), the temperature dependence of the magnetic susceptibility was measured and the results are presented in the form of $\chi_m T$ *versus* T curves (χ_m being the molar magnetic susceptibility per Cu^{II}–Ln^{III} unit and T the temperature). On the basis of $\chi_m T = f(T)$ curve profiles, the Cu^{II}–Ln^{III} compounds can be classified in two different categories depending on the involving lanthanide(III) ion. As shown in figure 4 for Cu^{II}–Ln^{III} (Ln = Ho (**1**), Tm (**2**), and Yb (**3**)), the values of $\chi_m T$ continuously decrease as temperature is lowered. At room temperature, the experimental values of $\chi_m T$, 13.74 (**1**), 6.87 (**2**), and 1.93 $cm^3\,Kmol^{-1}$ (**3**), respectively, are slightly smaller than the theoretical ones 14.43 (**1**), 7.51 (**2**), and 2.95 $cm^3\,Kmol^{-1}$ (**3**), respectively, expected for uncorrelated spin combination $(\chi_m T = \left((N\beta^2/3k)\left[g_{Cu}^2 S_{Cu}(S_{Cu}+1) + g_{Ln}^2 J_{Ln}(J_{Ln}+1)\right]\right))$. The $\chi_m T$ decreases by lowering the temperature to 7.24 for **1**, 2.73 for **2**, and 1.13 $cm^3\,Kmol^{-1}$ for **3**, respectively, at 1.8 K.

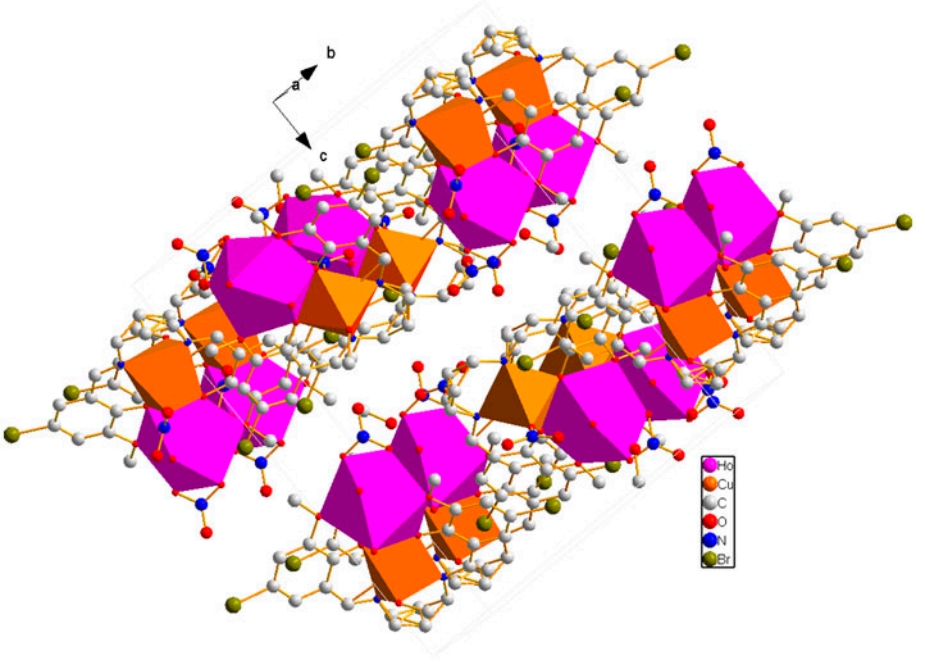

Figure 3. View of molecular layers perpendicular to *c* crystallographic axis in crystal structure of **1**.

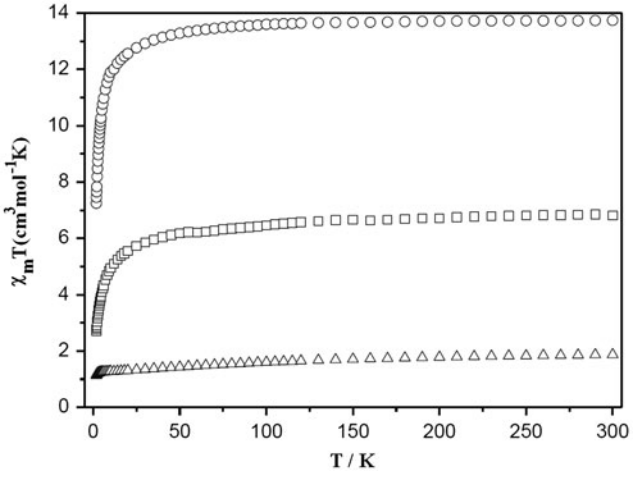

Figure 4. Temperature dependence of experimental $\chi_m T$ *vs.* T for **1** (○), **2** (□), and **3** (Δ).

The reduction of $\chi_m T$ values at low temperature could mainly arise from the crystal field splitting of Ln^{III} ions and/or contribution of the overall antiferromagnetic interactions among the metal ions. The nature of the interactions between Ln^{III} and Cu^{II} cannot be extracted due to the complicated magnetic paths and the orbital angular moment of the Ln^{III}

Table 4. Intermolecular interaction parameters in **1–3** (Å, °).

D–H···A	D–H	H···A	D···A	<DHA	Complex
O5–H5A···O18	0.97	1.69	2.65(1)	172	**1**
O5–H5B···O11	0.87	1.93	2.78(1)	166	**1**
O7–H7B···O17	0.96	1.83	2.74(1)	157	**1**
O7–H7A···O12^{i}	0.90	1.79	2.68(1)	170	**1**
O17–H17···O16^{ii}	0.82	2.07	2.87(1)	165	**1**
O6–H6A···O13^{i}	0.85	1.85	2.69(1)	166	**1**
O6–H6B···O14	0.85	2.03	2.75(1)	142	**1**
O18–H18···O16^{iii}	0.82	2.09	2.91(1)	171	**1**
C3–H3···O12^{ii}	0.93	2.49	3.41(1)	168	**1**
C7–H7···O10^{iv}	0.93	2.59	3.48(1)	162	**1**
C18–H18B···C15^{ii}	0.96	2.86	3.72(1)	150	**1**
C16···Cg(C5–C6)^{ii}	–	–	3.53(1)	–	**1**
O5–H5A···O18	0.95	1.72	2.67(1)	172	**2**
O5–H5B···O11	0.86	1.95	2.79(1)	167	**2**
O7–H7B···O17	0.94	1.81	2.74(1)	167	**2**
O7–H7A···O12^{i}	0.88	1.84	2.69(1)	163	**2**
O17–H17···O16^{ii}	0.85	2.10	2.91(1)	160	**2**
O6–H6A···O13^{i}	0.85	1.86	2.70(1)	171	**2**
O6–H6B···O14	0.85	2.05	2.75(1)	140	**2**
O18–H18···O16^{iii}	0.81	2.17	2.91(1)	151	**2**
C3–H3···O12^{ii}	0.93	2.51	3.43(1)	167	**2**
C7–H7···O10^{iv}	0.93	2.60	3.50(1)	164	**2**
C18–H18B···C15^{ii}	0.96	2.86	3.72(1)	151	**2**
C16···Cg(C5–C6)^{ii}	–	–	3.53(1)	–	**2**
O5–H5A···O18	0.78	2.20	2.89(1)	149	**3**
O5–H5B···O11	0.86	2.10	2.77(1)	136	**3**
O7–H7B···O17	0.95	1.77	2.71(1)	179	**3**
O7–H7A···O12^{i}	0.88	1.87	2.68(1)	151	**3**
O17–H17···O16^{ii}	0.82	2.12	2.90(2)	158	**3**
O6–H6A···O13^{i}	0.86	1.86	2.68(1)	159	**3**
O6–H6B···O14	0.86	1.98	2.76(1)	148	**3**
O18–H18···O16^{iii}	0.82	2.12	2.92(2)	164	**3**
C3–H3···O12^{ii}	0.93	2.52	3.43(1)	165	**3**
C7–H7···O10^{iv}	0.93	2.57	3.48(2)	166	**3**
C18–H18B···C15^{ii}	0.96	2.82	3.70(2)	152	**3**
C16···Cg(C5–C6)^{ii}	–	–	3.53	–	**3**

Note: Symmetry codes: ^{i} $x-1, y, z$; ^{ii} $-x+1/2, y+1/2, -z+1/2$; ^{iii} $x+1, y, z$; ^{iv} $x+1/2, -y+1/2, z+1/2$.

ions. Similar magnetic behavior was already reported for other Cu^{II}–Ln^{III} systems [2, 4, 6, 7, 46–49]. The $M=f(H)$ curves (figure 5) show a slow increase with applied field to reach magnetization at 5 T equal only to 6.27 for **1**, 4.17 for **2**, and 2.33 μ_B for **3**, respectively. The understanding of magnetic interactions involving rare earth(III) ions in molecular magnets is still far from satisfactory. The key point is the role of the orbital contribution, which introduces many complications, in particular large anisotropies.

For Cu^{II}–Lu^{III} (**4**), $\chi_m T$ is essentially constant in the whole temperature range and equal to 0.506 cm^3Kmol^{-1} (figure 6). The Lu^{III} ion is diamagnetic and Cu^{II} ions are too far from each other to interact significantly in the crystal lattice. Therefore, the magnetic susceptibility follows the Curie law expected for one isolated Cu^{II} ion [50]. The magnetization curve for Cu^{II}–Lu^{III} measured at 2 K was reproduced with the Brillouin function for one independent $S=1/2$ system (figure 6, see inset) and confirms our previous assumption.

As shown in table 5, in the series of heterodinuclear compounds Cu^{II}–Ln^{III} derived from BMSPDA and the heavier lanthanides with more than seven f electrons, the metal centers in the Cu^{II}–Gd^{III}, Cu^{II}–Tb^{III}, Cu^{II}–Dy^{III}, and Cu^{II}–Er^{III} complexes are ferromagnetically coupled, so the observations reported by us previously [10, 14] agree with the theoretical

Table 5. Comparison of selected structural parameters (bond distances in Å and angles in deg), and the nature of the magnetic exchange interactions of dinuclear Cu^{II}–Ln^{III} complexes derived from BMSPDA and other diphenoxo-bridged Schiff base ligands (where (a)–(g) data from the literature given under the table 5).

	Gd	**Tb**	**Dy**	**Ho**	**Er**	**Tm**	**Yb**
Cu^{II}–Ln^{III}	(a)	(a)	(a)	This work	(a)	This work	This work
Cu–O_{phen}	1.955(1)	1.951(2)	1.951(2)	1.952(3)	1.949(2)	1.954(4)	1.953(6)
	1.993(2)	1.995(2)	1.983(2)	1.983(3)	1.983(2)	1.991(4)	1.976(6)
Ln–O_{phen}	2.387(2)	2.372(2)	2.365(2)	2.351(3)	2.341(2)	2.338(4)	2.315(7)
	2.398(1)	3.378(2)	3.369(2)	2.356(3)	3.349(2)	2.344(4)	2.318(6)
Cu···Ln	3.539(1)	3.522(4)	3.618(1)	3.504(1)	3.613(1)	3.494(1)	3.476(1)
δ	2.5(1)	2.6(1)	2.9(1)	2.7(1)	2.8(1)	3.0(2)	2.9(4)
Exch. inter.	F	F	F	?	F	?	?
Cu^{II}–Ln^{III}	(b)	(c)	(c)	(c)	(c)	(c)	(c)
Cu–O_{phen}	1.899(8)	1.908(6)	1.902(2)	1.915(9)	*n.a.*	1.904(6)	1.887(8)
	1.903(9)	1.909(7)	1.899(2)	1.908(10)	*n.a.*	1.899(7)	1.897(9)
Ln–O_{phen}	2.330(8)	2.334(6)	2.318(2)	2.383(9)	*n.a.*	2.270(7)	2.282(8)
	2.403(8)	2.381(6)	2.375(6)	2.371(9)	*n.a.*	2.339(6)	2.323(9)
Cu···Ln	3.401	3.402	3.383	3.372	*n.a.*	3.347	3.338
δ	4.3	4.2	4.0	4.7	*n.a.*	4.1	4.3
Exch. inter.	F	F	F	F	?	F	F
Cu^{II}–Ln^{III}	(d)	(e)	(e)	(e)	(e)		
Cu–O_{phen}	1.953(2)	1.963(2)	1.956(2)	1.960(2)	1.9566(18)	–	–
	1.952(2)	1.958(2)	1.958(2)	1.955(2)	1.9513(17)	–	–
Ln–O_{phen}	2.387(2)	2.3797(19)	2.372(2)	2.358(2)	2.3495(17)	–	–
	2.390(2)	2.3771(19)	2.362(2)	2.356(2)	2.3464(17)	–	–
Cu···Ln	3.5231(4)	3.5177(18)	3.510(4)	3.499(2)	3.4923(19)	–	–
δ	16.6(2)	17.33	17.32	17.42	17.50	–	–
Exch. inter.	F	F	F	F	F	–	–
Cu^{II}–Ln^{III}	(f)	(g)		(g)	(g)		(g)
Cu–O_{phen}	1.915(2)	1.899(4)	–	1.897(2)	1.907(4)	–	1.913(3)
	1.909(2)	1.895(4)	–	1.883(2)	1.881(4)	–	1.895(3)
Ln–O_{phen}	2.380(2)	2.329(4)	–	2.294(4)	2.290(4)	–	2.259(3)
	2.343(2)	2.312(4)	–	2.292(4)	2.290(4)	–	2.253(3)
Cu···Ln	3.401	3.3276(8)	–	3.2936(5)	3.281	–	3.260
δ	2.1	18.4	–	17.6	19.1	–	19.1
Exch. inter.	F	F	–	F	F	–	AF

Notes: δ – dihedral angle between the $O1_{phen}$–Cu–$O2_{phen}$ and $O1_{phen}$–Ln–$O2_{phen}$ planes; Exch. inter. – Exchange interactions, n.a. data not available; (a) $[CuLn(L)(NO_3)_2(H_2O)_3MeOH]NO_3{\cdot}MeOH$ (Ln = Gd, Tb, Dy, Er) (Cristóvão *et al.* [14] and [10]); (b) $[CuLn(L^1)(NO_3)_3]$ (Ln = Gd) (Mohanta *et al.* [42]); (c) $[CuLn(L^1)(NO_3)_3]$ (Ln = Tb–Yb) (Koner *et al.* [3]); (d) $[Cu^{II}(L^4)(C_3H_6O)Ln^{III}(NO_3)_3]$ (Ln = Gd) (Costes *et al.* [43]); (e) $[Cu^{II}(L)(C_3H_6O)Ln^{III}(NO_3)_3]$ (Ln = Ho–Er) (Ishida *et al.* [44]); (f) $[Cu(H_2O)L^1Gd(NO_3)_3]$ (Koner *et al.* [45], Jana *et al.* [7]); and (g) $[CuLLn(NO_3)_3]$ (Ln = Tb−Yb) Jana *et al.* [7]).

prediction of Kahn *et al.* [2]. In the case of Cu^{II}–Ho^{III} (**1**), Cu^{II}–Tm^{III} (**2**), and Cu^{II}–Yb^{III} (**3**) complexes, no definite conclusion could be drawn. The nature of the magnetic exchange interactions between copper(II) and lanthanide(III) ions in the series of heterodinuclear compounds Cu^{II}–Ln^{III} was compared with the couplings in similar diphenoxo-bridged Schiff base complexes reported by Mohanta *et al.* [42], Costes *et al.* [43], Ishida *et al.* [44], Koner *et al.* [3, 45] and Jana *et al.* [7]. As shown in table 5, the metal ions in all Cu^{II}–Gd^{III}, Cu^{II}–Tb^{III}, and Cu^{II}–Dy^{III} complexes are coupled ferromagnetically. In contrast to the observed ferromagnetic interaction in the diphenoxo-bridged complexes Cu^{II}–Ho^{III} (reported by Koner *et al.* [3], Jana *et al.* [7] and Ishida *et al.* [44]), as well as in the Cu^{II}–Tm^{III} and Cu^{II}–Yb^{III} compounds (reported by Koner *et al.* [3]), no conclusion can be drawn regarding the magnetic interaction in the heterodinuclear complexes Cu^{II}–Ho^{III} (**1**), Cu^{II}–Tm^{III} (**2**), and Cu^{II}–Yb^{III} (**3**) derived from BMSPDA. As summarized in table 5, the metal centers in the

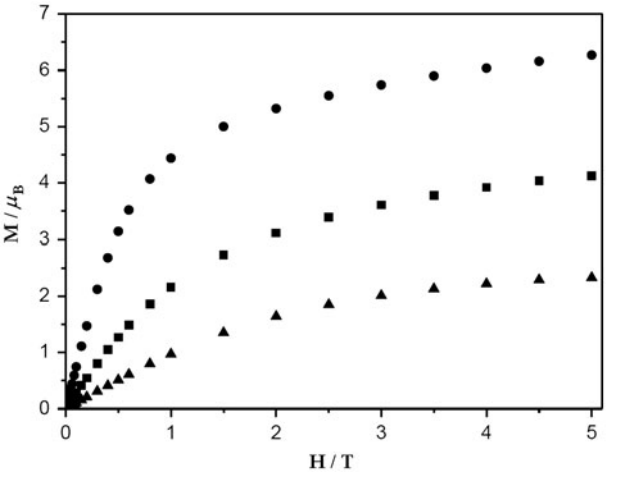

Figure 5. Field dependence of the magnetization for **1** (●), **2** (■), and **3** (▲) at 2 K.

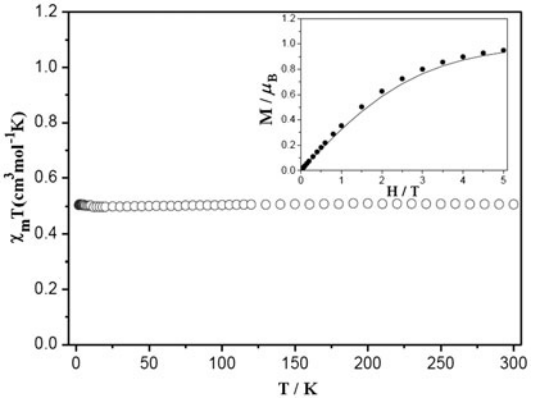

Figure 6. Temperature dependence of experimental $\chi_m T$ *vs.* T for **4** (○). The inset shows field dependence of the magnetization for **4** (●) at 2 K (the solid line is the Brillouin function curve for a one independent $S = 1/2$ of Cu^{II}–Lu^{III} unit).

dinuclear Schiff base Cu^{II}–Er^{III} complexes reported by us [10], Jana *et al.* [7] and Ishida *et al.* [44], are coupled ferromagnetically, while in the case of the Cu^{II}–Er^{III} compound investigated by Koner *et al.* [3], no definite conclusion could be reached.

The values of dihedral angle (δ) between $O1_{phen}$–Cu–$O2_{phen}$ and $O1_{phen}$–Ln–$O2_{phen}$ planes are presented in table 5. According to the literature, exchange interaction in Cu^{II}–Ln^{III} compounds is governed by the dihedral angle (δ). The higher the value of this angle, the weaker coupling between metal centers should be expected. Superexchange contribution is assumed for complexes with a planar LnO_2Cu molecular fragment [3, 7]. The δ values in the complexes derived from BMSPDA were in the range of 2.5(1)°–3.0(2)°, and the bridging moiety was almost planar or slightly twisted as in the compounds reported by Mohanta *et al.* [42] and Koner *et al.* [3] ($\delta = 4.0$–$4.7°$). In the other complexes, the bridging

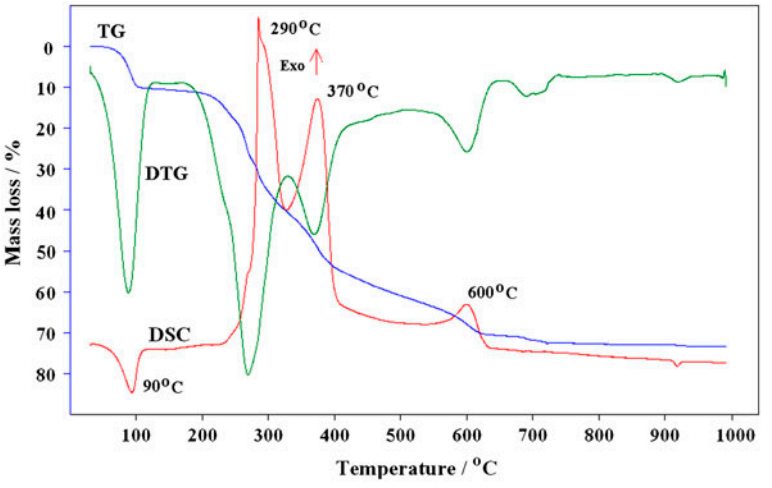

Figure 7. TG, DTG, and DSC curves of Cu^{II}–Ho^{III} (**1**) in air.

fragment is significantly twisted ($\delta = 16.6$–$19.1°$) and the magnetic exchange interactions are expected to be weaker compared to those in compounds reported by us [10, 14 and here], Mohanta *et al.* [42] and Koner *et al.* [3].

3.4. *Thermal analysis*

The thermal analyses of **1–4** were carried out by the TG/DSC (air) and TG/FTIR (argon) techniques (figures 7–9). The studied complexes are isostructural, and their decomposition processes proceed in similar ways. During heating of samples in air, the first change in mass estimated from recorded TG curves (10.80% (**1**), 11.20% (**2**), 10.70% (**3**), 11.00% (**4**), theoretical 11.45% (**1**), 11.40% (**2**), 11.36% (**3**), 11.34% (**4**)) from 65 to 170 °C corresponded to simultaneous loss of water and methanol. This process was accompanied by endothermic effect seen on the DSC curves with maximum at 90 °C (figure 7). In argon, the corresponding

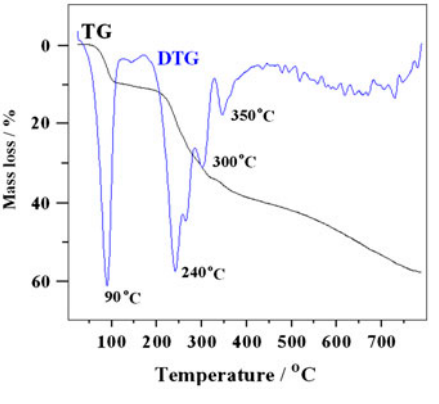

Figure 8. TG and DTG curves of Cu^{II}–Ho^{III} (**1**) in argon.

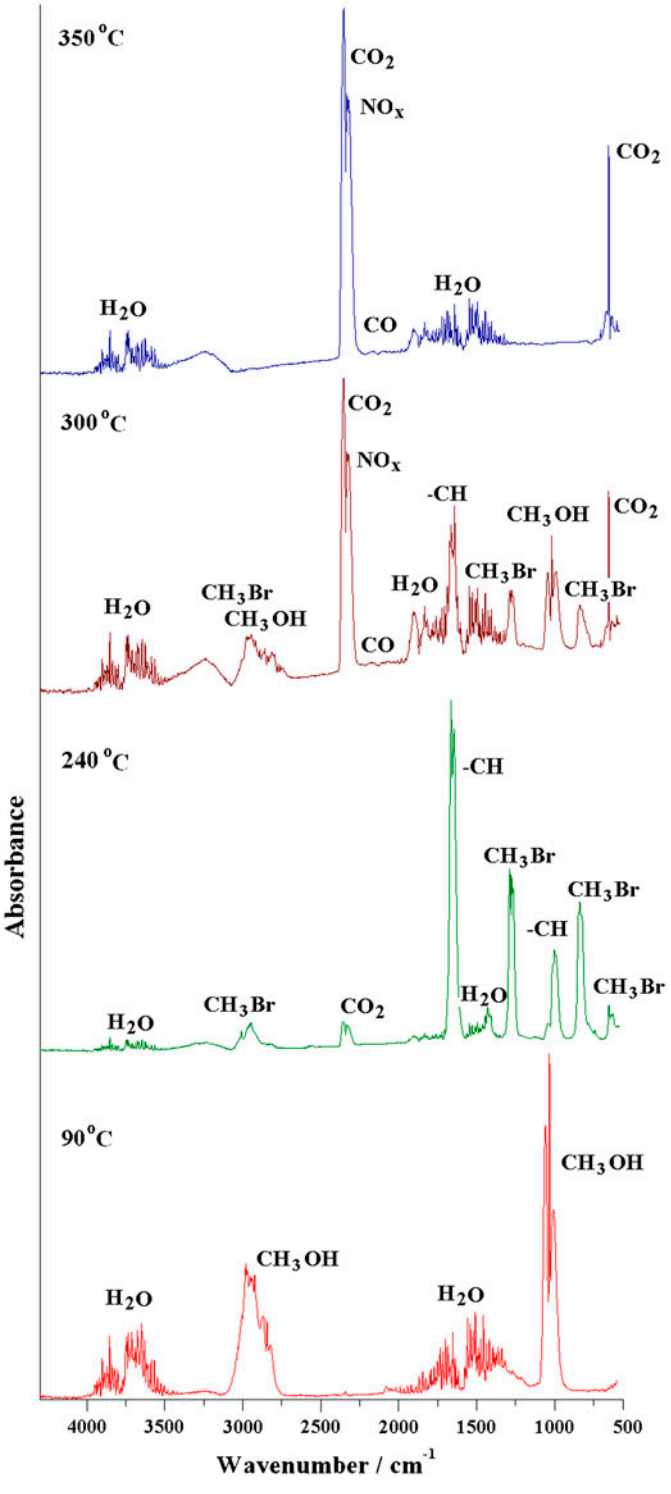

Figure 9. FTIR spectra of gaseous products of Cu^{II}–Ho^{III} (**1**) decomposition in argon.

mass losses calculated from TG curves had similar values: 11.20% (**1**), 10.80% (**2**), 11.00% (**3**), and 11.10% (**4**), respectively, indicating that the first stage of complex decomposition was the same in both conditions. FTIR spectra of the evolved gas phase confirmed that H_2O and CH_3OH are the main volatiles released during this stage (figure 9). The characteristic bands in the wavenumber ranges of 4000–3400 cm^{-1} and 2060–1260 cm^{-1} corresponded to stretching and deforming vibrations of water molecules, whereas the bands observed at the wavenumbers 3150–2750 cm^{-1} and 1100–950 cm^{-1} were characteristic of methanol molecules [21, 51–58]. In air, the degradation of the complexes at higher temperature was accompanied by strong exothermic effect recorded on DSC curves with maximum peaks at 290, 370, and 600 °C, respectively, connected mainly with burning of the Schiff base ligand. The decomposition process of Cu^{II}–Ln^{III} compounds is intricate and it is difficult to distinguish intermediate solid products. The solid residues obtained during thermal decomposition of complexes in air (found 25.69–27.00, theoretical 26.04–26.76%,) were probably a mixture of Cu^{II} and Ln^{III} oxides.

As shown in figure 9, the main volatiles emitted during decomposition at 240 °C (the maximum point of the DTG curve) were identified generally as aromatic and aliphatic compounds. The recorded FTIR spectra above 300 °C showed the characteristic doublet bands at 2240–2400 cm^{-1} and 669 cm^{-1}, respectively, assigned to stretching and deformation vibrations of CO_2 molecules. Characteristic bands at 4000–3400 cm^{-1} and 2060–1260 cm^{-1} corresponded to stretching and deforming vibrations of H_2O molecules, respectively. The bands at 2060–2240 cm^{-1} were characteristic of CO molecules [21, 51–55].

4. Conclusion

The reported synthesis and characterization of heterodinuclear complexes Cu^{II}–Ln^{III} (Ln = Ho^{III}, Tm^{III}, Yb^{III}, and Lu^{III}) **1–4** complete the series of Cu^{II}–4f coordination compounds with *N,N′*-bis(5-bromo-3-methoxysalicylidene)propylene-1,3-diamine (BMSPDA). Depending on the synthesis and crystallization conditions, mono-, di-, tri-, or even tetranuclear complexes have been formed. These results illustrate the rich coordination architecture which can be generated using BMSPDA. Additionally, even at the same synthesis conditions the size of the Ln^{III} ion itself was the crucial factor determining the molecular structure of the complex. The trinuclear units Cu^{II}–Ln^{III}–Cu^{II} are observed for light rare earth ions (Ce^{III}–Eu^{III} ($n < 7$)) and binuclear units for heavy lanthanide ions (Gd^{III}–Lu^{III} ($n \geq 7$)). The heterotrinuclear compounds crystallize in the monoclinic space group *C*2/*c*, whereas the heterodinuclear in $P2_1/n$. **1–4** were stable at room temperature both in argon and air. The first change in mass estimated from TG curve corresponded to the loss of water and methanol molecules.

For the studied Cu^{II}–Ln^{III} (Ln = Ho^{III}, Tm^{III}, and Yb^{III}) ($n > 7$) compounds, the temperature dependence of the magnetic susceptibility was governed by two factors, the energy spectrum of the Stark components of Ln^{III} and the Cu^{II}–Ln^{III} interaction. It was not possible to conclude about the nature of the magnetic Cu^{II}–Ln^{III} interaction due to the crystal field effects. The Cu^{II}–Lu^{III} complex showed no significant interaction in connection with the diamagnetic lutetium(III) ion. In previously reported heterodinuclear compounds Cu^{II}–Ln^{III} (Ln = Gd^{III}, Tb^{III}, Dy^{III}, and Er^{III}) ($n \geq 7$), the metal centers are coupled by ferromagnetic interaction, whereas the heterotrinuclear complexes Cu^{II}–Ln^{III}–Cu^{II} (Ln = Ce, Pr, Nd) ($n < 7$) exhibited the antiferromagnetic properties. In order to predict the magnetic behavior

of a new coordination compound, many factors have to be taken into account, such as geometry of the Schiff base ligand, distance between 3d and 4f ions, the planarity of the central part of the molecule (the dihedral angle δ), type of transition metal and lanthanide (III) ions, presence of additional bridging or chelating ligands, etc. Therefore, there is still need for studying the structure and magnetic properties of new complexes in various systems including new ligands and all lanthanide(III) ions to gain knowledge about the correlations between molecular structure and magnetic properties.

Supplementary data

Crystallographic data for **1–3** have been deposited with the Cambridge Crystallographic Data Center: CCDC 976502, 976503, and 976504, respectively. These data can be obtained free of charge via www.ccdc.cam.ac.uk/data_request/cif, or by emailing data_request@ccdc.cam.ac.uk, or by contacting the Cambridge Crystallographic Data Center, 12 Union Road, Cambridge CB2 1EZ, UK; Fax: + 44 1223 336033.

References

[1] A. Bencini, C. Benelli, A. Caneschi, R.L. Carlin, A. Dei, D. Gatteschi. *J. Am. Chem. Soc.*, **107**, 8128 (1985).
[2] M. Andruh, I. Ramade, E. Codjovi, O. Guillou, O. Kahn, J.C. Trombe. *J. Am. Chem. Soc.*, **115**, 1822 (1993).
[3] R. Koner, H.H. Lin, H.H. Wei, S. Mohanta. *Inorg. Chem.*, **44**, 3524 (2005).
[4] J.-P. Costes, F. Dahan, A. Dupuis, J.-P. Laurent. *Chem. Eur. J.*, **4**, 1616 (1998).
[5] A. Elmali, Y. Elerman. *J. Mol. Struct.*, **737**, 29 (2005).
[6] M.L. Kahn, C. Mathonière, O. Kahn. *Inorg. Chem.*, **38**, 3692 (1999).
[7] A. Jana, S. Majumder, L. Carrella, M. Nayak, T. Weyhermueller, S. Dutta, D. Schollmeyer, E. Rentschler, R. Koner, S. Mohanta. *Inorg. Chem.*, **49**, 9012 (2010).
[8] X.-P. Yang, R.A. Jones, V. Lynch, M.M. Oye, A.L. Holmes. *Dalton Trans.*, 849 (2005).
[9] X.-P. Yang, R.A. Jones, W.-K. Wong, V. Lynch, M.M. Oye, A.L. Holmes. *Chem. Commun.*, **17**, 1836 (2006).
[10] B. Cristóvão, B. Miroslaw, J. Kłak. *Polyhedron*, **34**, 121 (2012).
[11] B. Cristóvão, B. Miroslaw. *Inorg. Chim. Acta*, **401**, 50 (2013).
[12] B. Cristóvão, J. Kłak, B. Miroslaw. *Polyhedron*, **43**, 247 (2012).
[13] B. Cristóvão, J. Kłak, R. Pełka, B. Miroslaw, Z. Hnatejko. *Polyhedron*, **68**, 180 (2014).
[14] B. Cristóvão, J. Kłak, B. Miroslaw, L. Mazur. *Inorg. Chim. Acta*, **378**, 288 (2011).
[15] B. Cristóvão, B. Miroslaw, J. Kłak. *Polyhedron*, **62**, 218 (2013).
[16] B. Cristóvão, R. Pełka, B. Miroslaw, J. Kłak. *Inorg. Chem. Commun.*, **46**, 94 (2014).
[17] Oxford Diffraction. *Xcalibur CCD System, CrysAlis Software System (Version 1.171)*, Oxford Diffraction Ltd, Oxfordshire (2009).
[18] R.C. Clark, J.S. Reid. *Acta Cryst.*, **A51**, 887 (1995).
[19] G.M. Sheldrick. *Acta Cryst.*, **A64**, 112 (2008).
[20] L.J. Farrugia. *J. Appl. Crystallogr.*, **32**, 837 (1999).
[21] A. Bartyzel. *J. Coord. Chem.*, **66**, 4292 (2013).
[22] R.K. Dubey, P. Baranwal, A.K. Jha. *J. Coord. Chem.*, **65**, 2645 (2012).
[23] M. Rasouli, M. Morshedi, M. Amirnasr, A.M.Z. Slawin, R. Randall. *J. Coord. Chem.*, **66**, 1974 (2013).
[24] G.-B. Li, X.-J. Hong, Z.-G. Gu, Z.-P. Zheng, Y.-Y. Wu, H.-Y. Jia, J. Liu, Y.-P. Cai. *Inorg. Chim. Acta*, **392**, 177 (2012).
[25] A.-N.M.A. Alaghaz, B.A. El-Sayed, A.A. El-Henawy, R.A.A. Ammar. *J. Mol. Struct.*, **1035**, 83 (2013).
[26] S.O. Bahaffi, A.A.A. Aziz, M.M. El-Naggar. *J. Mol. Struct.*, **1020**, 188 (2012).
[27] S. Yadav, M. Ahmad, K.S. Siddiqi. *Spectrochim. Acta Part A*, **98**, 240 (2012).
[28] A.A.A. Aziz, A.N.M. Salem, M.A. Sayed, M.M. Aboaly. *J. Mol. Struct.*, **1010**, 130 (2012).
[29] P. Bhowmik, K. Harms, S. Chattopadhyay. *Polyhedron*, **49**, 113 (2013).
[30] W. Ferenc, B. Bocian. *J. Therm. Anal. Calorim.*, **62**, 831 (2000).
[31] M.R. Rosenthal. *J. Chem. Educ.*, **50**, 331 (1973).
[32] C.C. Addison, D.W. Amos, D. Sutton, W.H.H. Hoyle. *J. Chem. Soc. (A)*, 808 (1967).
[33] K. Nakamoto. *Infrared and Raman Spectra of Inorganic and Coordination Compounds*, John Wiley & Sons, Toronto (1997).
[34] T. Gao, P.-F. Yan, G.-M. Li, J.-W. Zhang, W.-B. Sun, M. Suda, Y. Einga. *Solid State Sci.*, **12**, 597 (2010).
[35] A.A. Khandar, S.A. Hosseini-Yazdi, M. Khatamian, P. McArdle, S.A. Zarei. *Polyhedron*, **26**, 33 (2007).
[36] S. Yadav, M. Ahmad, K.S. Siddiqi. *Spectrochim. Acta, Part A*, **98**, 240 (2012).

[37] K. Binnemans, Y.G. Galyametdinov, R.V. Deun, D.W. Bruce, S.R. Collinson, A.P. Polishchuk, I. Bikchantaev, W. Haase, A.V. Prosvirin, L. Tinchurina, I. Litvinov, A. Gubajdullin, A. Rakhmatullin, K. Uytterhoeven, L.V. Meervelt. *J. Am. Chem. Soc.*, **122**, 4335 (2000).
[38] F.Z.C. Fellah, J.P. Costes, F. Dahan, C. Duhayon, G. Novitchi, J.P. Tuchagues, L. Vendier. *Inorg. Chem.*, **47**, 6444 (2008).
[39] Z.A. Taha, A.M. Ajlouni, K.A. Al-Hassan, A.K. Hijazi, A.B. Faiq. *Spectrochim. Acta, Part A*, **81**, 317 (2011).
[40] Z.A. Taha, A.M. Ajlouni, K.W. Al Momani, A.A. Al-Ghzawi. *Spectrochim. Acta, Part A*, **81**, 570 (2011).
[41] L. Vaiana, M. Mato-Iglesias, D. Esteban-Gómez, C. Platas-Iglesias, A. de Blas, T. Rodríguez-Blas. *Polyhedron*, **29**, 2269 (2010).
[42] S. Mohanta, H.-H. Lin, C.-J. Lee, H.-H. Wei. *Inorg. Chem. Commun.*, **5**, 585 (2002).
[43] J.-P. Costes, F. Dahan, A. Dupuis, J.-P. Laurent. *Inorg. Chem.*, **36**, 3429 (1997).
[44] T. Ishida, R. Watanabe, K. Fujiwara, A. Okazawa, N. Kojima, G. Tanaka, S. Yoshii, H. Nojiri. *Dalton Trans.*, 13609 (2012).
[45] R. Koner, G.-H. Lee, Y. Wang, H.-H. Wei, S. Mohanta. *Eur. J. Inorg. Chem.*, **8**, 1500 (2005).
[46] M.L. Kahn, T.M. Rajendiran, Y. Jeannin, C. Mathonière, O. Kahn. *C. R. Acad. Sci. Paris, Série IIc, Chimie: Chem.*, **3**, 131 (2000).
[47] N. Kerbellec, N. Mahé, O. Guillou, C. Daiguebonne, O. Cador, T. Roisnel, R.L. Oushoorn. *Inorg. Chim. Acta*, **358**, 3246 (2005).
[48] Q.-D. Liu, S. Gao, J.-R. Li, B.-Q. Ma, Q.-Z. Zhou, K.-B. Yu. *Polyhedron*, **21**, 1097 (2002).
[49] R.L. Oushoorn, K. Boubekeur, P. Batail, O. Guillou. *Bull. Soc. Chim Fr.*, **133**, 777 (1996).
[50] O. Kahn. *Molecular Magnetism*, VCH, Weinheim (1993).
[51] X. Jiang, C. Li, Y. Chi, J. Yan. *J. Hazard. Mater.*, **173**, 205 (2010).
[52] T. Xu, X. Huang. *Fuel*, **89**, 2185 (2010).
[53] X. Jiang, C. Li, T. Wang, B. Liu, Y. Chi, J. Yan. *J. Anal. Appl. Pyrolysis*, **84**, 103 (2009).
[54] M. Sun, X.-X. Ma, Q.-X. Yao, R.-C. Wang, Y.-X. Ma, G. Feng, J.-X. Shang, L. Xu, Y.-H. Yang. *Energy Fuels*, **25**, 1140 (2011).
[55] L. Tao, G.-B. Zhao, J. Qian, Y.-K. Qin. *J. Hazard. Mater.*, **175**, 754 (2010).
[56] A.A.A. Aziz, A.N.M. Salem, M.A. Sayed, M.M. Aboaly. *J. Mol. Struct.*, **1010**, 130 (2012).
[57] T. Rosu, E. Pahontu, C. Maxim, R. Georgescu, N. Stanica, A. Gulea. *Polyhedron*, **30**, 154 (2011).
[58] S.O. Bahaffi, A.A.A. Aziz, M.M. El-Naggar. *J. Mol. Struct.*, **1020**, 188 (2012).